SynArtifact: Classifying and Alleviating Artifacts in Synthetic Images via Vision-Language Model

Bin Cao [1 2 3]   **Jianhao Yuan** [4]   **Yexin Liu** [3]   **Jian Li** [5]   **Shuyang Sun** [4]   **Jing Liu** [1 2]   **Bo Zhao** [3]

Abstract

In the rapidly evolving area of image synthesis, a serious challenge is the presence of complex artifacts that compromise perceptual realism of synthetic images. To alleviate artifacts and improve quality of synthetic images, we fine-tune Vision-Language Model (VLM) as artifact classifier to automatically identify and classify a wide range of artifacts and provide supervision for further optimizing generative models. Specifically, we develop a comprehensive artifact taxonomy and construct a dataset of synthetic images with artifact annotations for fine-tuning VLM, named SynArtifact-1K. The fine-tuned VLM exhibits superior ability of identifying artifacts and outperforms the baseline by 25.66%. To our knowledge, this is the first time such end-to-end artifact classification task and solution have been proposed. Finally, we leverage the output of VLM as feedback to refine the generative model for alleviating artifacts. Visualization results and user study demonstrate that the quality of images synthesized by the refined diffusion model has been obviously improved. The dataset is available at https://github.com/BBBiiinnn/SynArtifact

1. Introduction

The field of image synthesis has witnessed remarkable advancements, primarily driven by the development of generative models (Zhang et al., 2023a; Ho et al., 2020; Ramesh et al., 2022; Saharia et al., 2022a). These models have found widespread applications across various domains, including art creation, medical imaging, and autonomous driving. Despite this progress and applications, the quality of synthetic images still does not align with human preference perfectly.

Some related works (Xu et al., 2023; Huang et al., 2023) employ reward-driven methods to optimize generative models for improving the quality of synthetic images. However, most existing methods mainly depend on some single-score evaluation metrics of synthetic images. Utilizing single-score metric for optimizing generative models exhibits the inherent limitation, lacking the ability to reflect the diversity and complexity of artifacts directly, a significant issue that undermines the quality and perceptual realism of synthetic images. For example, a human annotator probably assigns the same score to a synthetic image with different kinds of artifacts, for example an image featuring distorted fingers (**Distortion**) while another image featuring six fingers (**Duplication**). Consequently, such less-informative annotations lead to ineffective attempt of automatically alleviating distortion and duplication in synthetic images.

The main challenge of artifact classification is the diversity and complexity of artifacts. To address this, we first develop a comprehensive taxonomy of common artifacts found in images synthesized by various generative models and construct a dataset with human-annotated artifact categories, captions and coordinates of artifacts, named SynArtifact-1K. The dataset is utilized for fine-tuning Vision-Language Model (VLM) to classify a wide range of artifacts. Experimental results show that the VLM fine-tuned on SynArtifact-1K surpasses the baseline by 25.66% of classification accuracy and 29.01% of F1 score. To alleviate artifacts, we improve the generative model by leveraging output of artifact classifier as the AI feedback, namely, Reinforcement Learning from AI Feedback (RLAIF) (Bai et al., 2022). Extensive results verify that the fine-tuned VLM can serve as the artifact classifier providing guidance for optimizing diffusion models. Our main contributions can be summarized as follows:

- We design a comprehensive artifact taxonomy for synthetic images including 13 kinds of artifacts, and propose the first image-with-artifact dataset, named SynArtifact-1K. The dataset contains 1.3k annotated images generated by various generative models, and each image is annotated with categories, captions and coordinates of artifacts.

- We demonstrate that VLM fine-tuned on SynArtifact-

---

[1]Institute of Automation, Chinese Academy of Sciences [2]School of Artificial Intelligence, University of Chinese Academy of Sciences [3]Beijing Academy of Artificial Intelligence [4]University of Oxford [5]YouTu Lab, Tencent. Correspondence to: Bo Zhao <bozhaonanjing@gmail.com>.
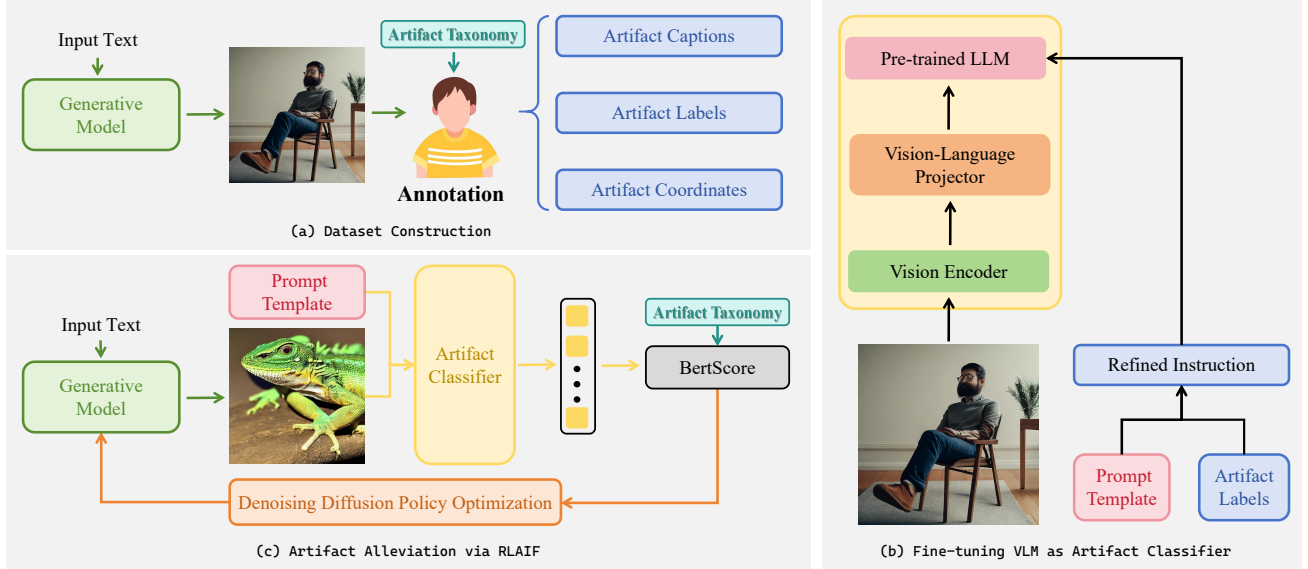
Figure 1. **The Proposed Method.** The entire pipeline consists of three components: dataset construction (see Section 3.2), fine-tuning VLM as artifact classifier (see Section 3.3) and artifact alleviation via RLAIF (see Section 3.4).

1K outperforms the baseline by 25.66% of classification accuracy and 29.01% of F1 score, showing the ability to identify artifacts and provide supervision for optimizing diffusion models.

• We exploit output of the fine-tuned VLM, namely, artifact classifier, as the supervision to refine the diffusion model in the manner of RLAIF. Extensive experiments demonstrate the refined diffusion model produces higher-quality images with less artifacts.

2. Related Work

2.1. Synthetic Image Assessment

Inception Score (IS) (Salimans et al., 2016) and Fréchet Inception Distance (FID) (Heusel et al., 2017) are widely-used automatic evaluation metrics for evaluating the performance of generative models. Both can only measure the feature distance between real and synthetic images. However, several related works reveal that IS and FID do not align with human preferences (Wu et al., 2023; Kirstain et al., 2023). AGIQA-1K (Zhang et al., 2023b) constructs a text-to-image dataset with human preference and conducts synthetic image quality evaluation through MOS (Mean Opinion Score). Pick-a-Pic (Kirstain et al., 2023) trains a CLIP-based score function (Radford et al., 2021) for predicting human preferences. HPSv2 (Wu et al., 2023) utilizes ChatGPT to rewrite prompts from DiffusionDB (Wang et al., 2022) and tunes CLIP through minimizing KL-divergence between the CLIP Score and human preference. ImageReward (Xu et al., 2023) employ BLIP (Li et al., 2022) as backbone and MLP head

to predict comparison of synthetic images. However, these methods for assessing synthetic images overlook artifacts and primarily focus on scoring or ranking.

Another line of works focus on the text-to-image alignment evaluation. CLIP Score (Hessel et al., 2021) computes cosine similarity between image embedding and text embedding as the metric for text-to-image alignment. T2I-CompBench (Huang et al., 2023) is a comprehensive benchmark for text-to-image generation, evaluating text-to-image alignment from 3 categories including attribute binding, object relationship and complex compositions. GENEVAL (Ghosh et al., 2023) proposes an object-focused framework for evaluating count, color and position of objects, leveraging object detection models. Previous object-level text-to-image alignment evaluation methods (Ghosh et al., 2023) (Cho et al., 2023) utilize detection model or segmentation model. In our work, we attempt to construct an end-to-end framework for artifact classification without any object detection models.

2.2. Assessment with Vision-Language Model

Vision-Language Models have achieved successful progress in recent years (Chen et al., 2023a; Zhu et al., 2023; Liu et al., 2023b;a; Chen et al., 2023b), especially integrating with LLMs (Large Language Models) (Zheng et al., 2023; Touvron et al., 2023). X-IQE (Chen, 2023) utilizes MiniGPT-4 (Zhu et al., 2023) and designs a hierarchical CoT (Chain of Thought) (Wei et al., 2022) to generate text for assessment. The entire CoT includes fidelity evaluation,
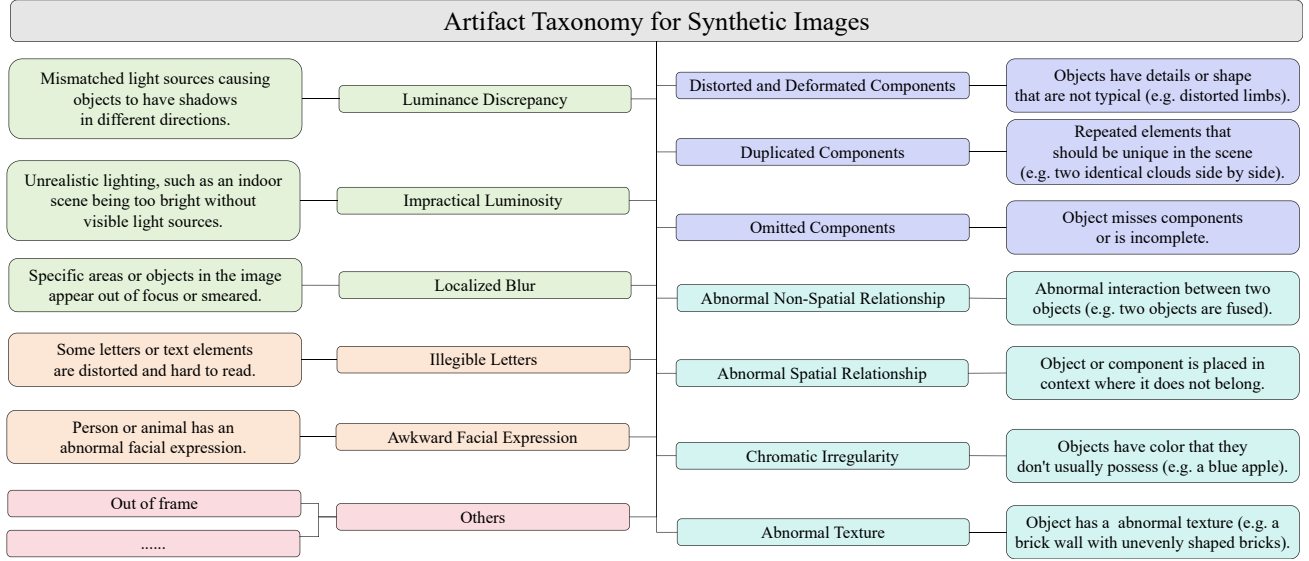
Artifact Taxonomy for Synthetic Images

Mismatched light sources causing objects to have shadows in different directions.	Luminance Discrepancy		Distorted and Deformated Components	Objects have details or shape that are not typical (e.g. distorted limbs).
Unrealistic lighting, such as an indoor scene being too bright without visible light sources.	Impractical Luminosity		Duplicated Components	Repeated elements that should be unique in the scene (e.g. two identical clouds side by side).
Specific areas or objects in the image appear out of focus or smeared.	Localized Blur		Omitted Components	Object misses components or is incomplete.
Some letters or text elements are distorted and hard to read.	Illegible Letters		Abnormal Non-Spatial Relationship	Abnormal interaction between two objects (e.g. two objects are fused).
Person or animal has an abnormal facial expression.	Awkward Facial Expression		Abnormal Spatial Relationship	Object or component is placed in context where it does not belong.
Out of frame /	Others		Chromatic Irregularity	Objects have color that they don't usually possess (e.g. a blue apple).
			Abnormal Texture	Object has a abnormal texture (e.g. a brick wall with unevenly shaped bricks).

Figure 2. **Artifact Taxonomy.** The entire artifact taxonomy contains 13 kinds of artifacts. Each kind of artifact is accompanied with explanation.

alignment evaluation, and aesthetic evaluation. Each evaluation task consists of an image description, task-specific analysis, and scoring. TIFA (Hu et al., 2023) uses GPT-3 (Mann et al., 2020) to generate question-answer pairs filtered by a QA model. Then, the VQA accuracy is the metric for faithfulness between the synthetic image and text prompt. VPEval (Cho et al., 2023) defines five kinds of image generation skills, including object, count, spatial scale, and text rendering. Subsequently, it designs a series of specialized modules for assessment. DepictQA (You et al., 2023) breaks through the constraints of score-based methods, leveraging Multi-modal Language Models for image quality evaluation. However, DepictQA (You et al., 2023) utilizes a reference image for comparison. In our work, we aim to construct a artifact classification model without reference.

2.3. Reinforcement Learning from AI Feedback

Reinforcement Learning from Human Feedback (RLHF) (Ouyang et al., 2022), which fine-tunes language models towards human preference, is initially adopted in natural language processing (NLP). However, this method needs massive expert-annotated model outputs, which remains time-consuming and challenging. Reinforcement Learning from AI Feedback (RLAIF) is first introduced in (Bai et al., 2022), which provides a promising alternative. Lee et al. (Lee et al., 2023) demonstrates RLAIF can achieve comparable performance to RLHF on summarization, helpful dialogue generation, and harmless dialogue generation through experiments. In this paper, we employ RLAIF to guide the optimization of diffusion model online.

3. Methodology

3.1. Overview

Figure 1 gives an overview of our approach. To classify and alleviate artifacts, we first employ diffusion model to generate synthetic images and annotate images under the guidance of a comprehensive artifact taxonomy resulting in artifact labels, captions and coordinates. Next, we convert artifact labels into visual instruction utilizing the prompt template. Then, we employ visual instructions to fine-tune VLM as artifact classifier. Finally, leveraging output of fine-tuned VLM, namely, artifact classifier, as AI feedback, *BertScore* between output of artifact classifier and each kind of artifact is calculated as artifact classification reward. Diffusion model is optimized by maximizing artifact classification reward to alleviate artifacts through Denoising Diffusion Policy Optimization (DDPO) (Black et al., 2023).

3.2. Dataset Construction

3.2.1. ARTIFACT TAXONOMY

While substantial advancements have been achieved in generative models, the synthetic images still struggle to align with human preferences. Moreover, the artifacts, which compromise quality of synthetic images, remain common in synthetic images. Therefore, as the first step of alleviating artifacts, we analyze and categorize various types of artifacts presented in synthetic images.

We construct a comprehensive taxonomy of artifacts, as shown in Figure 2. In the coarse-grained classification, arti-

Table 1. **Sources of Prompts and Synthetic Images.** Prompts are sampled from image-caption datasets and user input. We employ diffusion model to generated images.

Prompt Source	Generative Model	#Images
ImageNet	Stable Diffusion v2.1	100
MSCOCO	Stable Diffusion v2.1	200
DrawBench	Stable diffusion v1.0	40
DrawBench	Stable diffusion v1.4	40
DrawBench	Stable diffusion v1.5	40
DrawBench	Stable diffusion v2.0	40
DrawBench	Stable diffusion v2.1	40
ImageReward	Stable Diffusion	400
Midjourney Users	Stable Diffusion v2.1	210
DALLE-3 Users	DALLE-3	200

Figure 3. **Our Annotation Paradigm.** Each synthetic image is annotated with coordinates, label and caption of artifacts.

Figure 4. **Distribution of Artifact Annotation.** Distortion, omission, and duplication are dominant artifacts while artifacts related to lighting are infrequent.

facts can be categorized into four groups w.r.t. *object-aware*, *object-agnostic*, *lighting*, and *others*. The popular object-aware related artifacts include illegible letters which are hard to recognize, and awkward facial expressions of humans and animals. Object-agnostic related artifacts contain two sub-categories: abnormal components and attribute mis-binding. Abnormal components related artifacts mainly focus on three issues: distortion, omission and duplication regardless of the object type. For example, a popular omission is that human has fewer fingers or limbs without any specification. Attribute mis-binding, such as color, texture, and spatial position of different objects, also frequently emerges as a significant challenge for generative models. For example, the model may generate an object with the strange color that does not align with the common sense while the color is not mentioned in the text prompt. Finally, we also pay attention to lighting and blur, which is also a noteworthy problem causing the unreality of synthetic images.

3.2.2. IMAGE GENERATION AND ANNOTATION

Prompt Collection and Image Generation. To ensure the diversity of prompts and corresponding synthetic images, we collect and select prompts from three sources. Firstly, partial prompts are sampled from image-caption datasets, including ImageNet (Deng et al., 2009), COCO captions (Chen et al., 2015). Secondly, a number of prompts are user input of Midjourney and DALLE-3 (Betker et al., 2023). Then, we use Stable Diffusion v2.1 (Rombach et al., 2021) to generate images. We also sample synthetic images collected by previous works, such as HPSv2 (Wu et al., 2023) (We only utilize image generated from DrawBench (Saharia et al., 2022b)) and ImageReward (Xu et al., 2023). Finally, we construct a dataset containing 1.3K text-image pairs, which is summarized in Tab.1.

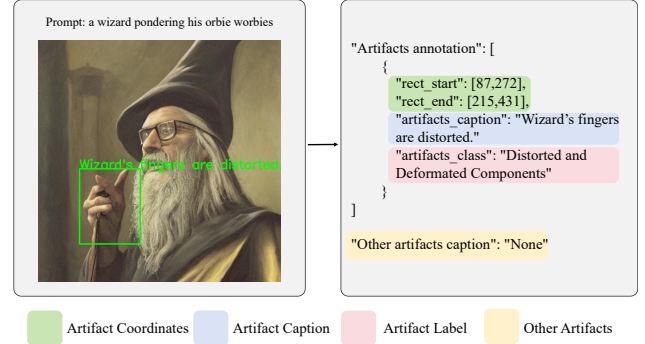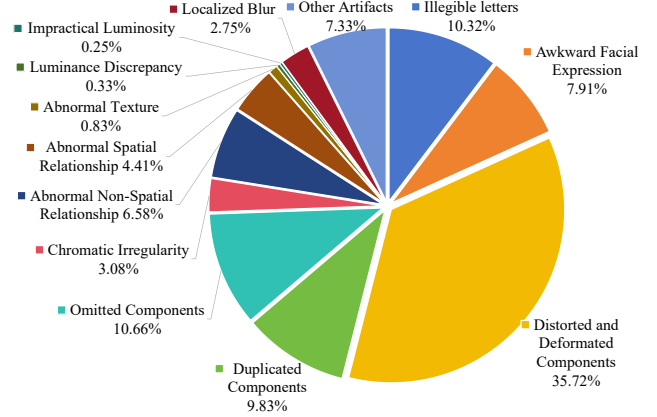**Human Annotation and Analysis.** Previous annotation paradigms primarily focus on global scoring and ranking images (Xu et al., 2023; Wu et al., 2023; Kirstain et al., 2023; Li et al., 2023), providing limited information for alleviating artifacts. Our annotation paradigm is shown in Figure 3. The annotation includes labels (see Section 3.2.1), coordinates, and captions (detailed descriptions) of artifacts. Recognizing the challenge of locating all artifacts, we additionally utilize captions to describe other unspecified artifacts. Following the above annotation paradigm, we construct a dataset consisting of 768 images with artifacts and 542 images without artifacts, called SynArtifact-1K. The distribution of artifact annotation is illustrated in Figure 4, showing that distortion is the predominant type of artifacts and luminosity is relatively infrequent. This imbalance could arise from both the weakness of generative model and the biased distribution of human prompts.
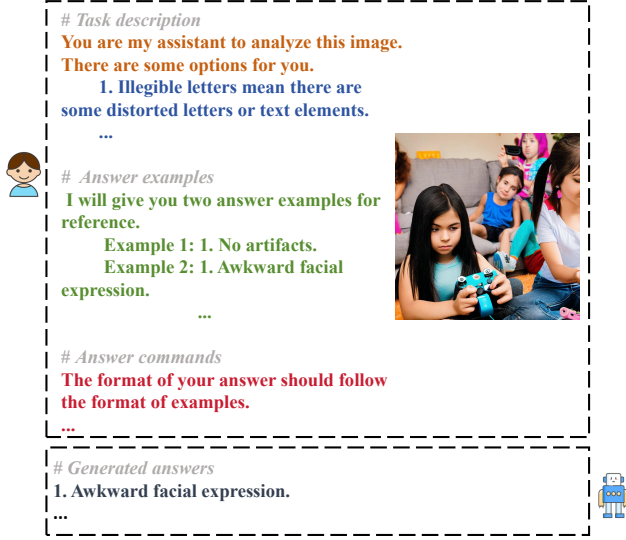
Figure 5. **Question-Answer Template for Artifact Classification.** The template includes a set of options. Each option is accompanied with a detailed explanation. Reference answers are used to ensure the standardized format for response.

3.3. Automatic Artifact Classification via Fine-tuning Vision-Language Model

To fine-tune VLM as artifact classifier utilizing SynArtifact-1K, we design a prompt template to transform various types of artifacts into instructions facilitating fine-tuning VLM, as shown in Figure 5. In accordance with Section 3.2.1, we consider 13 types of artifacts. Initially, we approach artifact classification as multiple binary classification tasks, designing a question for each kind of artifact. Every answer can only be *"Yes"* or *"No"*. However, since a synthetic image typically contains a few kinds of artifacts, most answers of questions are *"No"*, leading to imbalance within answers. After fine-tuning, we observe that VLM tends to answer *"No"*. To address this imbalance, we modify our approach to adopt a single question-answer pair for artifact classification, only answering types of artifacts in synthetic image rather than posing questions about each kind of artifact individually. Based above analysis, we consider artifact classification as a multi-label classification task. Our text prompt is designed as follow:

Task description → Presenting all options
→ Answer examples → Answer commands

By presenting all available options with detailed explanations, VLM selects one or more options for response. Additionally, we also provide two reference answers and answer commands to ensure the standardized response format and avoid in-context conflicts, as shown in Figure 5.

In our work, we employ LLaVA (Liu et al., 2023a;b)

$\Phi_{\text{VLM}}(\cdot, \cdot)$ utilized for artifact classification, which contains a vision encoder $\Phi_{\theta_v}(\cdot)$, a pre-trained large language model $\Phi_{\theta_l}(\cdot)$ and a vision-language projector $\Phi_{\theta_c}(\cdot)$. Given a synthetic image x_v and a question x_q, the vision encoder extracts image features $f_v = \Phi_{\theta_v}(x_v)$ and the vision-language projector convert image features into the word embedding space. Subsequently, the vision and language tokens are concatenated and fed into LLM to generate answers:

$$\tilde{x}_a = \Phi_{\theta_l}(x_q, \Phi_{\theta_c}(f_v)) \tag{1}$$

The cross entropy loss is calculated between generated answers $\tilde{x}_a$ and ground truth x_a to update parameters of vision-language projector θ_c and LLM θ_l:

$$\theta_l^*, \theta_c^* = \underset{\theta_l, \theta_c}{\operatorname{argmin}} \mathcal{L}_{CE}(\tilde{x}_a, x_a) \tag{2}$$

3.4. Artifact Classification as AI Feedback for Alleviating Artifact

Based on the developed artifact alleviation pipeline (see Figure 1), we further investigate reinforcement learning from AI feedback to improve the quality of synthetic images. For this purpose, we design a reward function reflecting the defined "human" perception of artifacts in images. This reward function is then employed to fine-tune the text-to-image generative model (i.e., latent diffusion model (Rombach et al., 2021)) through online reinforcement learning to reduce the occurrence of artifacts in synthetic images. Several works (Black et al., 2023; Fan et al., 2023; Wallace et al., 2023) have demonstrated the effectiveness of policy gradient optimization-based reinforcement learning for diffusion model fine-tuning, which provides better maximization of human reward (Fan et al., 2023) and preference alignment (Wallace et al., 2023).

Specifically in our application, we adopt the Denoising Diffusion Policy Optimization (DDPO) (Black et al., 2023) to fine-tune Stable Diffusion (Rombach et al., 2022). This involves a delicate reward function design of converting the discrete artifact classifier output into a continuous and informative artifact-aware reward for an effective estimate of policy gradient for optimization.

$$\nabla_\theta \mathcal{J} = \mathbb{E}[\sum_{t=0}^{T} \frac{p_\theta(x_{t-1} \mid x_t, c)}{p_{\theta_{\text{old}}}(x_{t-1} \mid x_t, c)} \\ \nabla_\theta \log p_\theta(x_{t-1} \mid x_t, c) \, r(x_v, c)] \tag{3}$$

As indicated in Equation (3), the policy gradient $\nabla_\theta \mathcal{J}$ is estimated with an expectation over multiple denoising steps x_t in diffusion process with importance sampling. The reward function $r(x_v, c)$ is designed as in Equation (4):

Table 2. **Artifact Classification Experiments.** We ablate multiple design choices, including fine-tuning dataset, weight initialization and updating LLM. In all experiments, the vision encoder is frozen while the vision-language projector is tuned. **Stage 1** denotes we load the **pre-trained** weights of LLaVA-v1.5 as the initialization. **Stage 2** denotes we load the **visual instruction-tuned** weights of LLaVA-v1.5 as the initialization. Note that fine-tuning on LLaVA-v1.5-mix665K results in the vanilla LLaVA-v1.5, which is the baseline.

Fine-tuning Dataset	Weight Initialization	Updating LLM	Categories	Accuracy	Precision	Recall	F1 Score
LLaVA-v1.5-mix665K	Stage 1	✓	All	20.00	25.28	22.14	23.01
			Distortion	-	-	-	-
			No artifacts	55.09	46.67	43.75	45.16
SynArtifact-1K	Stage 1	✗	All	**45.66**	**54.40**	**51.84**	**52.02**
			Distortion	**71.70**	**63.08**	**44.57**	**52.23**
			No artifacts	**65.66**	**55.74**	**91.07**	**69.15**
	Stage 1	✓	All	36.23	48.87	47.30	46.50
			Distortion	62.26	46.92	66.30	54.95
			No artifacts	63.40	55.56	66.96	60.73
	Stage 2	✗	All	34.34	39.87	42.30	40.10
			Distortion	57.74	36.84	30.43	33.33
			No artifacts	53.58	46.99	76.79	58.31

$$r(x_v, c) = \text{BertScore}(''\text{No artifacts}'', \Phi_{\text{VLM}}(x_v, x_q))$$
$$- \alpha \sum_{k}^{N} \text{BertScore}(s_k, \Phi_{\text{VLM}}(x_v, x_q)) + \beta, \quad (4)$$

where Φ_{VLM} is our artifact classifier, and x_v is the denoised synthetic image and x_q is question for our artifact classifier during fine-tuning. We adopt *BertScore* (Zhang et al., 2019) to measure the similarity between the output of our artifact classifier $\Phi_{\text{VLM}}(x_v, x_q)$ and a set of pre-defined phrases of artifact class s_k (see Section 3.2.1), where k is the index of artifact category. The reward function encourages the generative model to produce images with "*No artifacts*" while penalizing the overall weighted sum of each artifact. The weight coefficient α and offset β are set to ensure a positive reward function.

4. Experiments

4.1. Dataset & Setting

We divide SynArtifact-1K into a training set, comprising 1045 annotated images, and a testing set, containing 265 annotated images. We employ LLaVA-v1.5-7B (Liu et al., 2023a;b) and fine-tune it for experiments. For artifact classification, we conduct comprehensive ablation studies on fine-tuning dataset, weight initialization, updating LLM. For artifact classification, the batch size is set to be 16. For fine-tuning Stable Diffusion v1.5, we adopt the LoRA (Hu et al., 2021) strategy and the prompts in ImageNet-animal[1]. We set the learning rate 3e-4 and the batch size 24.

---
[1]Detailed prompt list is available at https://github.com/kvablack/ddpo-pytorch

4.2. Artifact Classification Results

Comparison to Baseline. Recognizing the potential presence of multiple types of artifacts in a synthetic image, we consider the artifact classification as a multi-label classification task (see Section 3.3). The label space includes 13 kinds of artifacts (see Figure 2) and "*No artifacts*". Then, we evaluate the ability to identify artifacts on the testing set. As shown in Table 2, LLaVA, fine-tuned on SynArtifact-1K, demonstrates a remarkable ability in artifact classification and the accuracy reaches up to 45.66%, achieving a notable improvement of 25.66%, compared with the baseline LLaVA-v1.5 which is fine-tuned on LLaVA-v1.5-mix665K. Lacking synthetic images in LLaVA-v1.5-mix665K, LLaVA tends to categorize an input image as a normal image without artifacts. Instead, through fine-tuning on SynArtifact-1K, the accuracy of "*No artifacts*" further improves by 10.57% and showcases the enhanced ability to identify artifacts. Considering distortion is the most prevalent artifact, we also present the performance on this category in Table 2. The baseline LLaVA-v1.5 model performs extremely bad in identifying distortion in synthetic images, while ours achieve 52.23% F1 Score.

Updating LLM Parameters. As illustrated in Table 2, updating LLM parameters causes much worse performance. The potential reason is that the presented SynArtifact-1K dataset is small, tuning LLM on the small set will cause overfitting and thus worse performance.

Weight Initialization. Considering that LLaVA training process consists of two stages: feature alignment, i.e. pre-training (**Stage 1**) and visual instruction tuning (**Stage 2**), we conduct a comprehensive investigation on the impact
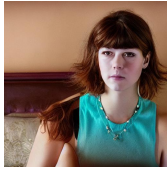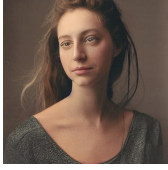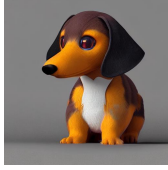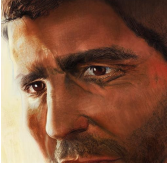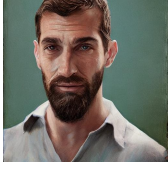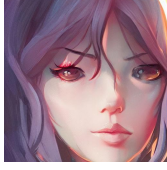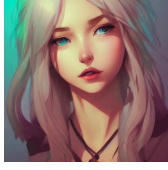
Prompt	Original Image	Artifact Alleviated Image	Prompt	Original Image	Artifact Alleviated Image
squishmallow , kawaii , of **cheese** , in the **snow** sky , 8k , 3D			a masterpiece portrait photo of a beautiful **young woman** who looks like a manic pixie dream girl mary elizabeth winstead, symmetrical face		
portrait of a beautiful **young woman**, front view. casual clothing. studio photo by annie leibovitz.			high quality 3 d render hyperrealist very cute very fluffy smooth **dachshund plush mascot**, photo from the side, multi pastel colors, vray, smooth background, artstation, ultra detailed		
portrait of a handsome **man** of 3 9 years old, green eyes, light brown, good looking, wide nose by david rutkowski, by artgem			portrait of a beautiful alt **girl**, art by lois van baarle and ross tran and sam yang and ilya kuvshinov and guweiz, digital art, high detail, sharp focus, unreal engine 5, trending on artstation, deviantart, pinterest, 4 k uhd image		

Figure 6. **Visualization of Samples in Reinforcement Learning from Artifact Classification.** Each example contains the prompt, synthetic image and artifact-alleviated image, showing that artifacts in synthetic image have been alleviated through DDPO.

of weight initialization for artifact classification. As shown in Table 2, we observe that fine-tuning LLaVA utilizing SynArtifact-1K based on Stage 1 achieves better performance. It is worth noting that fine-tuned model based on Stage 2 achieves a recall of 30.43% for *"Distortion"* but for a recall of 76.79% for *"No artifacts"*, indicating that model still tend to misclassify a synthetic image with distortion into a synthetic image without distorted components.

4.3. Primary Experiment on Artifact Detection

To locate artifacts, we further attempt to perform artifact detection. The chat template for artifact detection and implement details can be seen in Appendix A.3. The primary results of artifact detection are shown in Figure 7. LLaVA shows the primary ability to locate artifacts in synthetic images through fine-tuning on Synthetic-1K. To evaluate detection results quantitatively, we calculate IOU (Intersection Over Union) between the predicted bounding box and ground truth containing human annotated bounding boxes of the same kinds of artifacts. However, we observe that LLaVA struggles with precise artifact localization. The fined-tuned LLaVA tends to predict a large bounding box to include multiple artifacts. The potential reasons are that LLaVA lacks the ability of localization inherently and the presented SynArtifact-1K dataset is small. This observation underscores the challenge and potential of artifact detection task, which can develop more explainable quality
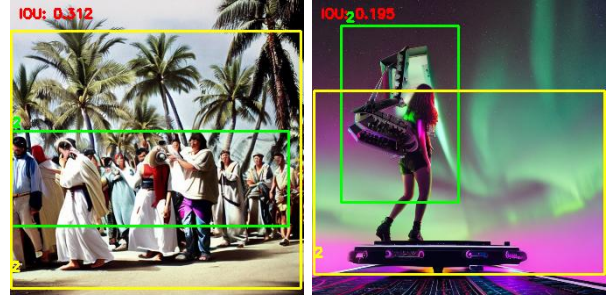

Figure 7. **Artifact Detection Results.** We present artifact detection results, with the ground truth, i.e. the human annotations in **Green**, and the detection results in **Yellow**. IOU is highlighted on the top-left of the image. The number at the left lower corner in the bounding box is the artifact category index, and category *"2"* denotes *"Distorted and deformed components"*.

evaluation metrics for synthetic images and provide valuable insights for optimizing diffusion models. In the future, Vision-Language Models with powerful visual grounding ability, such as Shikra (Chen et al., 2023b) and MiniGPT-v2 (Chen et al., 2023a), are also attempting.

4.4. Improved Generative Model with Artifact Alleviation

We further demonstrate the effectiveness and applicability of the artifact classifier for fine-tuning diffusion model. With
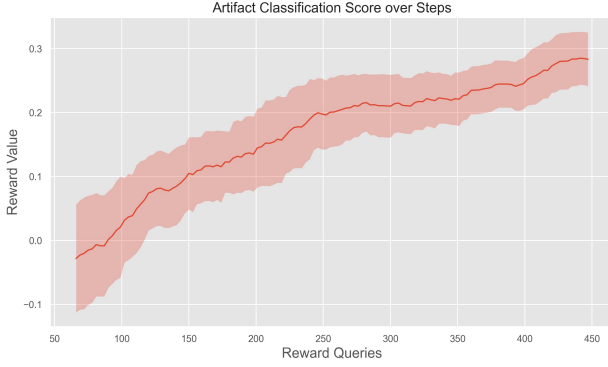
Figure 8. **Improving Artifact Classification Reward.** Synthetic images evaluated with the artifact classifier obtain increasing rewards with more queries from the artifact classifier, indicating fewer artifacts are presented.

the designed reward feedback (Section 3.4), Stable Diffusion produces higher quality synthetic images with higher artifact reward as shown in Figure 8. Note that our artifact classification reward increases quickly, indicating the efficiency of the DDPO strategy and the informativeness of the designed artifact score in reflecting the artifact presented in synthetic images.

Visualization. To better illustrate the effectiveness of reinforcement learning from the artifact classifier, comparison between synthetic images produced by base and fine-tuned diffusion model are present in Figure 6. We can observe clear alleviation and removal of several notable artifacts (i.e., distorted limbs, duplicated components, out of frame, and awkward facial expression) during the fine-tuning process. For example, the man who is out of frame (row 3, column 1) has been moved to the center of image and the dog whose head is incomplete (row 2, column 2) has been refined to a dog with perfect details.

User Study. To quantitatively evaluate artifact alleviation effects leveraging RLAIF, we recruit 18 well-educated volunteers to rate the synthetic images from 1 to 7 for the image quality. The results are shown in Figure 9. We can find that synthetic images generated by our tuned diffusion model can better align with human preference, indicating that RLAIF remains a beneficial impact in alleviating artifacts in synthetic images.

5. Limitations

In this section, we discuss some limitations of our work. SynArtifact-1K contains 1.3k text-image pairs and we recognize better artifact classification and alleviation performance could be achieved with the larger scale of dataset. While
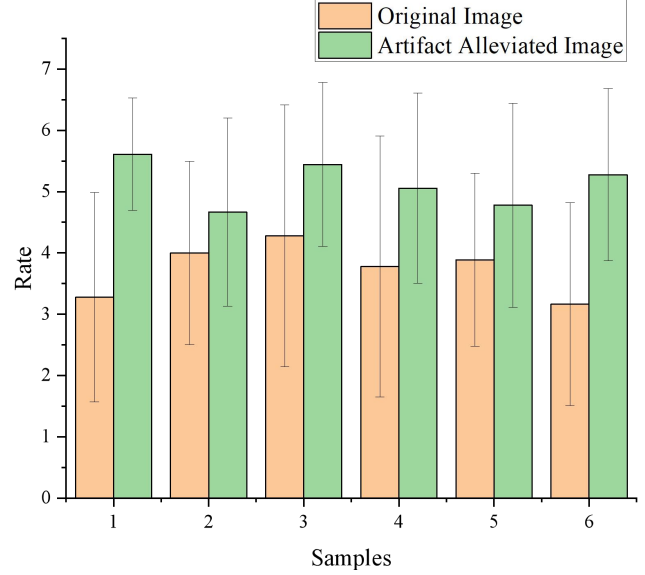

Figure 9. **User Study.** We present mean (**Histogram**) and variance (**Boxplot**) of human rate for original image and artifact alleviated image. Artifact alleviated images beat original images.

LLaVA serves as our foundation model that demonstrates artifact classification ability through fine-tuning, the artifact detection ability still needs improvements because LLaVA inherently lacks the detection ability. In the future work, the model with powerful detection ability is worth attempting.

6. Conclusion

In this paper, we focus on artifacts in synthetic images and address two key issues: artifact classification and alleviation. We construct a systematic artifact taxonomy involving 13 kinds of common artifacts, and create the first image-with-artifact dataset annotated with artifact categories, descriptions and coordinates, named SynArtifact-1K. A Vision Language Model is fine-tuned on SynArtifact-1K to automatically classify artifacts, and further used to refine the generative model in the manner of RLAIF. Extensive experiments of visualization and user study reveal that our method can effectively improve the quality of synthetic images.

References

Bai, Y., Kadavath, S., Kundu, S., Askell, A., Kernion, J., Jones, A., Chen, A., Goldie, A., Mirhoseini, A., McKinnon, C., et al. Constitutional ai: Harmlessness from ai feedback. *arXiv preprint arXiv:2212.08073*, 2022.

Betker, J., Goh, G., Jing, L., Brooks, T., Wang, J., Li, L., Ouyang, L., Zhuang, J., Lee, J., Guo, Y., et al. Improving image generation with better captions. *Computer Science.*

https://cdn. openai. com/papers/dall-e-3. pdf, 2:3, 2023.

Black, K., Janner, M., Du, Y., Kostrikov, I., and Levine, S. Training diffusion models with reinforcement learning. *arXiv preprint arXiv:2305.13301*, 2023.

Chen, J., Zhu, D., Shen, X., Li, X., Liu, Z., Zhang, P., Krishnamoorthi, R., Chandra, V., Xiong, Y., and Elhoseiny, M. Minigpt-v2: large language model as a unified interface for vision-language multi-task learning. *arXiv preprint arXiv:2310.09478*, 2023a.

Chen, K., Zhang, Z., Zeng, W., Zhang, R., Zhu, F., and Zhao, R. Shikra: Unleashing multimodal llm's referential dialogue magic. *arXiv preprint arXiv:2306.15195*, 2023b.

Chen, X., Fang, H., Lin, T.-Y., Vedantam, R., Gupta, S., Dollár, P., and Zitnick, C. L. Microsoft coco captions: Data collection and evaluation server. *arXiv preprint arXiv:1504.00325*, 2015.

Chen, Y. X-iqe: explainable image quality evaluation for text-to-image generation with visual large language models. *arXiv preprint arXiv:2305.10843*, 2023.

Cho, J., Zala, A., and Bansal, M. Visual programming for text-to-image generation and evaluation. In *NeurIPS*, 2023.

Deng, J., Dong, W., Socher, R., Li, L.-J., Li, K., and Fei-Fei, L. Imagenet: A large-scale hierarchical image database. In *2009 IEEE conference on computer vision and pattern recognition*, pp. 248–255. Ieee, 2009.

Fan, Y., Watkins, O., Du, Y., Liu, H., Ryu, M., Boutilier, C., Abbeel, P., Ghavamzadeh, M., Lee, K., and Lee, K. Dpok: Reinforcement learning for fine-tuning text-to-image diffusion models. *arXiv preprint arXiv:2305.16381*, 2023.

Ghosh, D., Hajishirzi, H., and Schmidt, L. Geneval: An object-focused framework for evaluating text-to-image alignment. *arXiv preprint arXiv:2310.11513*, 2023.

Hessel, J., Holtzman, A., Forbes, M., Bras, R. L., and Choi, Y. Clipscore: A reference-free evaluation metric for image captioning. *arXiv preprint arXiv:2104.08718*, 2021.

Heusel, M., Ramsauer, H., Unterthiner, T., Nessler, B., and Hochreiter, S. Gans trained by a two time-scale update rule converge to a local nash equilibrium. *Advances in neural information processing systems*, 30, 2017.

Ho, J., Jain, A., and Abbeel, P. Denoising diffusion probabilistic models. *Advances in neural information processing systems*, 33:6840–6851, 2020.

Hu, E. J., Shen, Y., Wallis, P., Allen-Zhu, Z., Li, Y., Wang, S., Wang, L., and Chen, W. Lora: Low-rank adaptation of large language models. *arXiv preprint arXiv:2106.09685*, 2021.

Hu, Y., Liu, B., Kasai, J., Wang, Y., Ostendorf, M., Krishna, R., and Smith, N. A. Tifa: Accurate and interpretable text-to-image faithfulness evaluation with question answering. *arXiv preprint arXiv:2303.11897*, 2023.

Huang, K., Sun, K., Xie, E., Li, Z., and Liu, X. T2i-compbench: A comprehensive benchmark for open-world compositional text-to-image generation. *arXiv preprint arXiv:2307.06350*, 2023.

Kirstain, Y., Polyak, A., Singer, U., Matiana, S., Penna, J., and Levy, O. Pick-a-pic: An open dataset of user preferences for text-to-image generation. *arXiv preprint arXiv:2305.01569*, 2023.

Lee, H., Phatale, S., Mansoor, H., Lu, K., Mesnard, T., Bishop, C., Carbune, V., and Rastogi, A. Rlaif: Scaling reinforcement learning from human feedback with ai feedback. *arXiv preprint arXiv:2309.00267*, 2023.

Li, C., Zhang, Z., Wu, H., Sun, W., Min, X., Liu, X., Zhai, G., and Lin, W. Agiqa-3k: An open database for ai-generated image quality assessment. *IEEE Transactions on Circuits and Systems for Video Technology*, pp. 1–1, 2023. doi: 10.1109/TCSVT.2023.3319020.

Li, J., Li, D., Xiong, C., and Hoi, S. Blip: Bootstrapping language-image pre-training for unified vision-language understanding and generation. In *International Conference on Machine Learning*, pp. 12888–12900. PMLR, 2022.

Liu, H., Li, C., Li, Y., and Lee, Y. J. Improved baselines with visual instruction tuning, 2023a.

Liu, H., Li, C., Wu, Q., and Lee, Y. J. Visual instruction tuning, 2023b.

Mann, B., Ryder, N., Subbiah, M., Kaplan, J., Dhariwal, P., Neelakantan, A., Shyam, P., Sastry, G., Askell, A., Agarwal, S., et al. Language models are few-shot learners. *arXiv preprint arXiv:2005.14165*, 2020.

Ouyang, L., Wu, J., Jiang, X., Almeida, D., Wainwright, C. L., Mishkin, P., Zhang, C., Agarwal, S., Slama, K., Ray, A., et al. Training language models to follow instructions with human feedback, 2022. *URL https://arxiv. org/abs/2203.02155*, 13, 2022.

Radford, A., Kim, J. W., Hallacy, C., Ramesh, A., Goh, G., Agarwal, S., Sastry, G., Askell, A., Mishkin, P., Clark, J., et al. Learning transferable visual models from natural language supervision. In *International conference on machine learning*, pp. 8748–8763. PMLR, 2021.

Ramesh, A., Dhariwal, P., Nichol, A., Chu, C., and Chen, M. Hierarchical text-conditional image generation with clip latents, 2022. *URL https://arxiv. org/abs/2204.06125*, 7, 2022.

Rombach, R., Blattmann, A., Lorenz, D., Esser, P., and Ommer, B. High-resolution image synthesis with latent diffusion models, 2021.

Rombach, R., Blattmann, A., Lorenz, D., Esser, P., and Ommer, B. High-resolution image synthesis with latent diffusion models. In *Proceedings of the IEEE/CVF conference on computer vision and pattern recognition*, pp. 10684–10695, 2022.

Saharia, C., Chan, W., Saxena, S., Li, L., Whang, J., Denton, E., Ghasemipour, S. K. S., Ayan, B. K., Mahdavi, S. S., Lopes, R. G., et al. Photorealistic text-to-image diffusion models with deep language understanding. *URL https://arxiv. org/abs/2205.11487*, 4, 2022a.

Saharia, C., Chan, W., Saxena, S., Li, L., Whang, J., Denton, E. L., Ghasemipour, K., Gontijo Lopes, R., Karagol Ayan, B., Salimans, T., et al. Photorealistic text-to-image diffusion models with deep language understanding. *Advances in Neural Information Processing Systems*, 35: 36479–36494, 2022b.

Salimans, T., Goodfellow, I., Zaremba, W., Cheung, V., Radford, A., and Chen, X. Improved techniques for training gans. *Advances in neural information processing systems*, 29, 2016.

Touvron, H., Lavril, T., Izacard, G., Martinet, X., Lachaux, M.-A., Lacroix, T., Rozière, B., Goyal, N., Hambro, E., Azhar, F., et al. Llama: Open and efficient foundation language models. *arXiv preprint arXiv:2302.13971*, 2023.

Wallace, B., Dang, M., Rafailov, R., Zhou, L., Lou, A., Purushwalkam, S., Ermon, S., Xiong, C., Joty, S., and Naik, N. Diffusion model alignment using direct preference optimization. *arXiv preprint arXiv:2311.12908*, 2023.

Wang, Z. J., Montoya, E., Munechika, D., Yang, H., Hoover, B., and Chau, D. H. DiffusionDB: A large-scale prompt gallery dataset for text-to-image generative models. *arXiv:2210.14896 [cs]*, 2022. URL https://arxiv.org/abs/2210.14896.

Wei, J., Wang, X., Schuurmans, D., Bosma, M., Xia, F., Chi, E., Le, Q. V., Zhou, D., et al. Chain-of-thought prompting elicits reasoning in large language models. *Advances in Neural Information Processing Systems*, 35: 24824–24837, 2022.

Wu, X., Hao, Y., Sun, K., Chen, Y., Zhu, F., Zhao, R., and Li, H. Human preference score v2: A solid benchmark for evaluating human preferences of text-to-image synthesis. *arXiv preprint arXiv:2306.09341*, 2023.

Xu, J., Liu, X., Wu, Y., Tong, Y., Li, Q., Ding, M., Tang, J., and Dong, Y. Imagereward: Learning and evaluating human preferences for text-to-image generation, 2023.

You, Z., Li, Z., Gu, J., Yin, Z., Xue, T., and Dong, C. Depicting beyond scores: Advancing image quality assessment through multi-modal language models. *arXiv preprint arXiv:2312.08962*, 2023.

Zhang, L., Rao, A., and Agrawala, M. Adding conditional control to text-to-image diffusion models. In *Proceedings of the IEEE/CVF International Conference on Computer Vision*, pp. 3836–3847, 2023a.

Zhang, T., Kishore, V., Wu, F., Weinberger, K. Q., and Artzi, Y. Bertscore: Evaluating text generation with bert. *arXiv preprint arXiv:1904.09675*, 2019.

Zhang, Z., Li, C., Sun, W., Liu, X., Min, X., and Zhai, G. A perceptual quality assessment exploration for aigc images. *arXiv preprint arXiv:2303.12618*, 2023b.

Zheng, L., Chiang, W.-L., Sheng, Y., Zhuang, S., Wu, Z., Zhuang, Y., Lin, Z., Li, Z., Li, D., Xing, E. P., Zhang, H., Gonzalez, J. E., and Stoica, I. Judging llm-as-a-judge with mt-bench and chatbot arena, 2023.

Zhu, D., Chen, J., Shen, X., Li, X., and Elhoseiny, M. Minigpt-4: Enhancing vision-language understanding with advanced large language models. *arXiv preprint arXiv:2304.10592*, 2023.

A. Appendix

A.1. SynArtifact-1K Samples.

In our work, the main contribution is to propose SynArtifact-1K, the first synthetic image dataset including artifact labels, captions and coordinates. Figure 10 shows examples of SynArtifact-1K. We can observe various kinds of artifacts in SynArtifact-1K, such as distorted hands, illegible letters and awkward facial expressions. Objects in SynArtifact-1K mainly contain human, animals and letters, which still remains challenging for generative models. Image styles in SynArtifact-1K are also various, such as art, realistic photos and movie poster. SynArtifact-1K can be utilized to classify and detect artifacts in synthetic images.
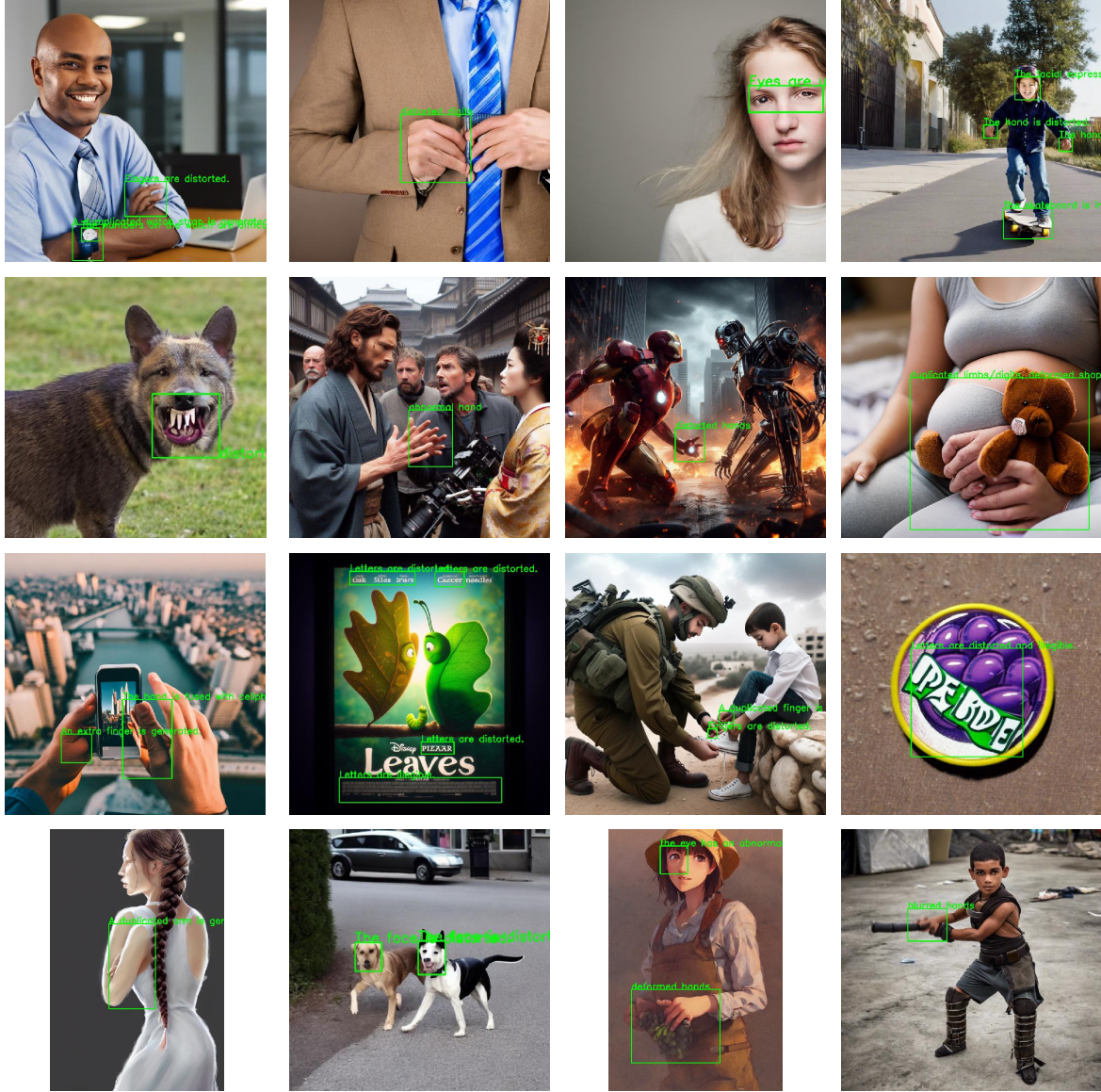
Figure 10. **Visualization of Samples of SynArtifact-1K.** Each synthetic image with artifacts is annotated with bounding box and caption. Then, annotator maps the artifact caption into artifact taxonomy in Figure 2.

A.2. Instruction for Artifact Classification.

Figure 11 shows complete instruction utilized for artifact classification. Instruction only contains one question-answer pair. We prompt Vision-Language Model with task description and all options. In order to standardize the format of answers, we

provide two answers examples. One answer template is about no artifacts and another template is about synthetic image with artifacts. Furthermore, we also provide some answer commands to avoid in-context conflict within answer i.e. the answer includes both some artifact labels and no artifacts.

Figure 11. **Instruction for Artifact Classification.** Instruction contains task description, all options, answer examples and answer commands. Answer only contains categories of artifacts in synthetic images.

A.3. Instruction for Artifact Detection.

Figure 12 exhibits complete instruction for artifact detection. We divide artifact detection into four sub-tasks: artifact judgement, artifact classification, artifact location and other artifacts. Artifact judgement could be only answered utilizing *"Yes"* or *"No"*. Artifact classification should be answered utilizing various kinds of artifacts in Figure 2. Furthermore, artifact location aims to locate artifacts that are selected in artifact classification using normalized coordinates $[x_1, y_1, x_2, y_2]$. Considering the image process in CLIP will crop image to 336×336, we resize synthetic image into 336×336 with padding and normalize annotated coordinates to make instruction align with images. Finally, other artifact caption is also needed. To evaluate the performance of artifact detection, we load the pre-trained weights of LLaVA-v1.5-7B as the initialization and fine-tune it with a learning rate of 2e-5.

 # Task description
You are my assistant to analyze whether artifacts exist in this image.

 # Question
Are there any artifacts in this image?

 # Generated answers
Yes, there are some artifacts in this image.

 # Task description
You are my assistant to analyze categories of artifacts in this image.

 # Question
There are some choices for you.
  1. Illegible letters mean there are some distorted letters or text elements.
  2. Awkward facial expression means person or animal has an abnormal facial expression.
  3. Distorted and deformed components mean objects having details or shape that are not typical (e.g. distorted limbs).
  4. Duplicated components mean repeated elements that should be unique in the scene (e.g. two identical clouds side by side).
  5. Omitted components mean object misses components or is incomplete.
  6. Chromatic irregularity means objects having colors that they don't usually possess (e.g. a blue apple).
  7. Abnormal non-spatial relationship means abnormal interaction between two objects (e.g. two objects are fused).
  8. Abnormal spatial relationship means object or component is placed in context where it does not belong.
  9. Abnormal texture means the texture of an object is abnormal (e.g. a brick wall with unevenly shaped bricks).
  10. Luminance discrepancy means mismatched light sources causing objects to have shadows in different directions.
  11. Impractical luminosity means unrealistic lighting, such as an indoor scene being too bright without visible light sources.
  12. Localized blur means specific areas or objects in the image appear out of focus or smeared.

 # Generated answers
Distorted and deformed components.Duplicated components.Omitted components.

 # Task description
You are my assistant to locate artifacts in this image.

 # Question
Please provide the coordinates for artifacts that you choose using the format of [x1,x2,y1,y2].

 # Generated answers
Distorted and deformated components: [0.112, 0.408, 0.29, 0.618].
Duplicated components: [0.203, 0.366, 0.288, 0.514].
Omitted components: [0.386, 0.274, 0.45, 0.347].

 # Task description
You are my assistant to analyze other artifacts in this image.

 # Question
Are there any other artifacts except the above in this image?

 # Generated answers
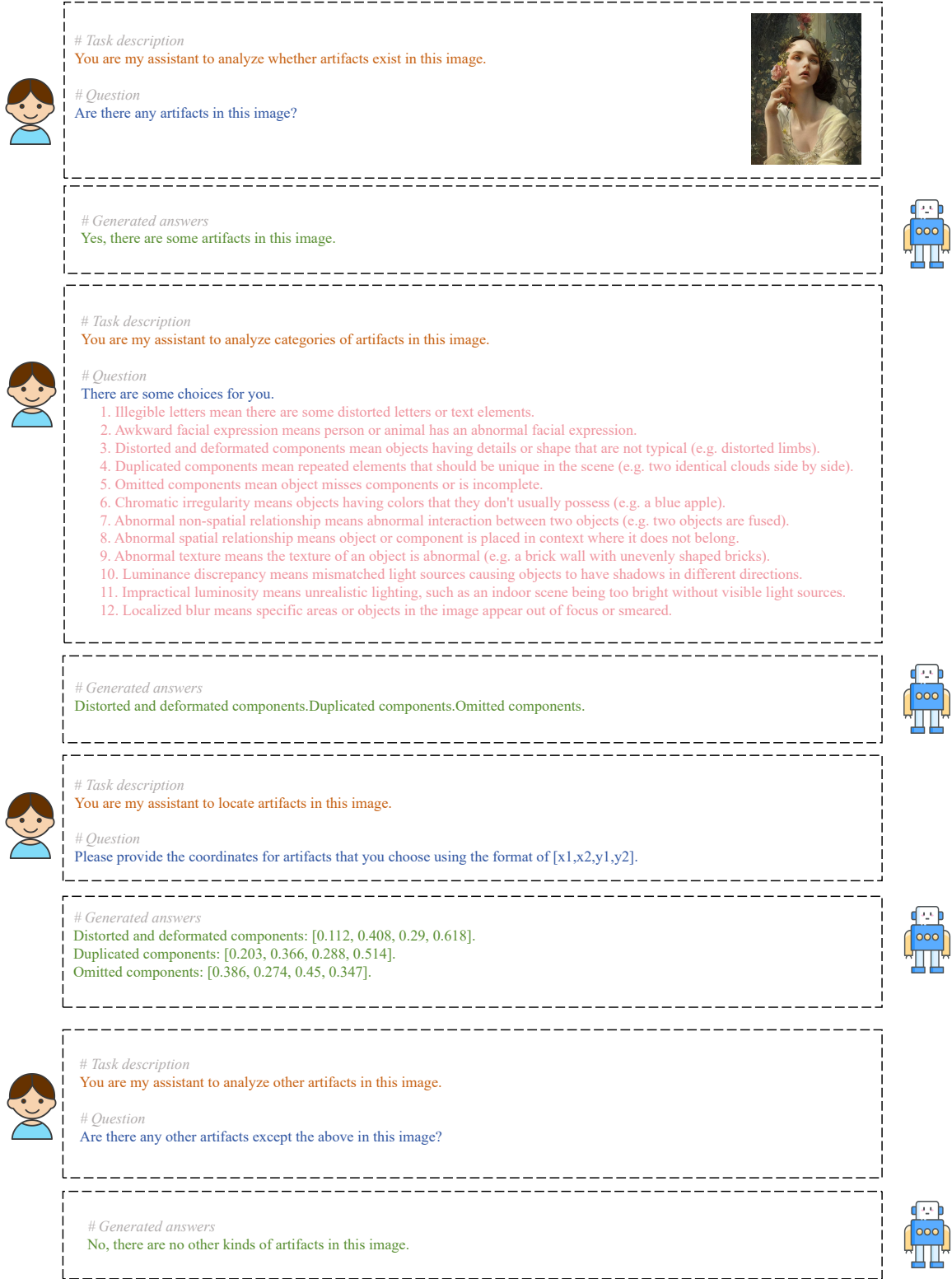No, there are no other kinds of artifacts in this image.

Figure 12. **Instruction for Artifact Detection.** Instruction contains artifact judgement, artifact classification, artifact location and other artifact. Artifact classification question contains task description and all options. Locate artifact using the format of $[x_1, y_1, x_2, y_2]$.

A.4. Artifact Alleviated Samples.

Figure 13 shows samples with the process of fine-tuning diffusion model leveraging output of artifact classifier. We can observe that some artifacts have been alleviated. For example, bear's duplicated ears vanish (**rows 2**) and the man who is out of frame has been refined into the center of photo (**rows 4**).
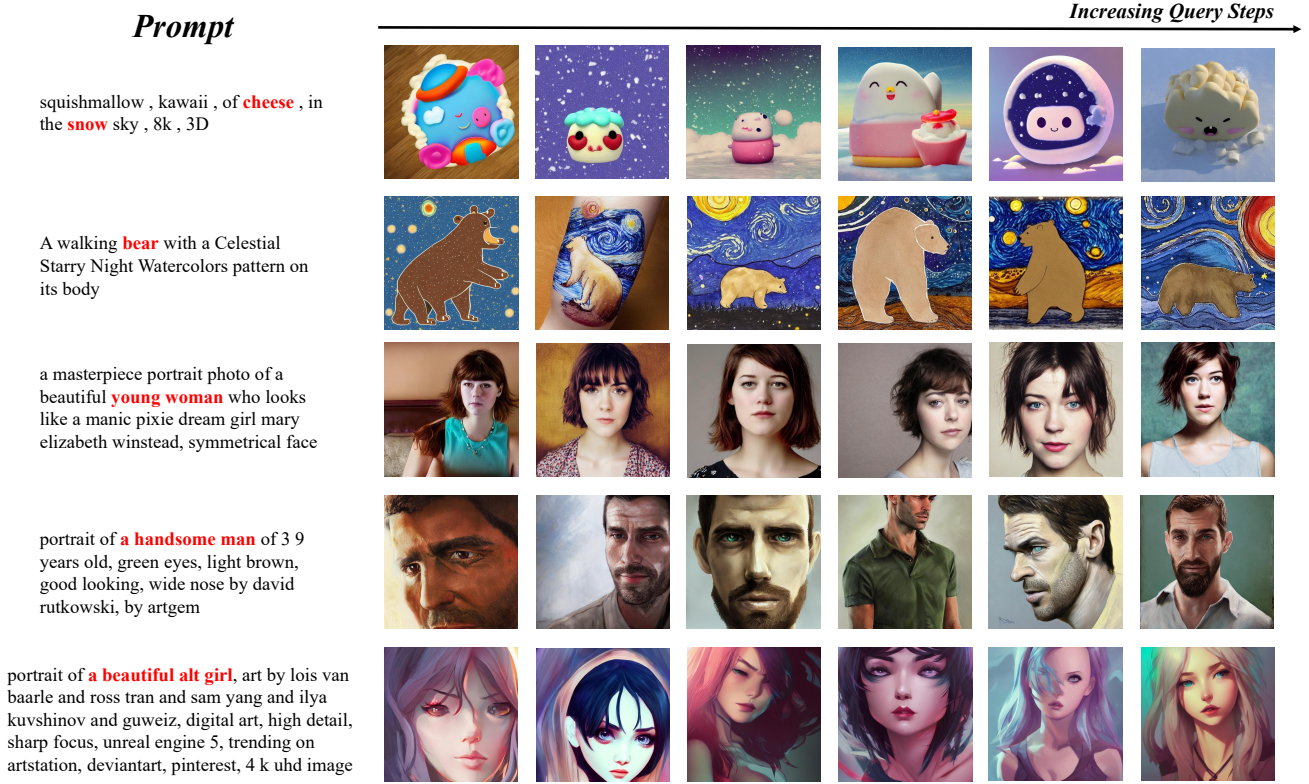

Figure 13. **Visualization of Samples in Reinforcement Learning from Artifact Classification.** The leftmost image is produced with base Stable Diffusion v1.5. From left to right, it indicates images with an increasing number of query steps and artifact score.